Mitigated Flux Attenuation of Ceramic Membrane Ultrafiltration Coupled with TiO₂ Photocatalytic Oxidation Pretreatment

[1]Zhou Zhen, [2]Yu Yaqin, [3]Yao Jilun, [1]Zhang Xing and [1]Ding Zhaoxia
[1]Department of Military Facilities, Army Logistics University of PLA, Chongqing 401311, China.
[2]State Key Laboratory of Environmental Chemistry and Ecotoxicology,
Research Center for Eco-Environmental Sciences, Chinese Academy of Sciences,
Beijing 100085, China.
[3]Engineering andf Technological Research Center of National Disaster Relief Equipment, Army
Logistics University of PLA, Chongqing 401311, China.
yjlun305@126.com*

Summary: To aggrandize membrane flux during micro-polluted surface water ultrafiltration process, TiO₂ photocatalytic oxidation pretreatment was conducted to mitigate the ultrafiltration membrane fouling. The single-factor experiments and membrane resistance analysis methods have shown that the water throughput performance in the hybrid process is affected by TiO₂ concentration, aeration rate, transmembrane pressure, and crossflow velocity. Subsequently, the orthogonal methodology was further conducted to optimize the overriding variables using membrane flux as the response value. Simultaneously, parallel of UF ceramic membrane performance between chemical coagulation and TiO₂ photocatalytic pretreatment was implemented and the excellent chemical washing method was determined. The results manifested that i) the impact on permeate flux was demonstrated following the order of the transmembrane pressure, crossflow velocity, aeration rate, and TiO₂ concentration. The statistical optimum operating condition was acquired at 0.5 g/L additional TiO₂, an aeration rate of 2 L/min, a transmembrane pressure of 0.15 MPa, and a crossflow velocity of 2.0 m/s; ii) TiO₂ photocatalytic oxidation buttressed UF flux was superior to chemical coagulation pretreatment; iii) The best cleaning performance in permeability recovery was exhibited in citric acid solution after 40 minutes cycle-cleaning.

Introduction

Admittedly, membrane technology can be elucidated as a physical sieve that winnows desired materials from admixture, shoved by the pressure gradient, temperature gradient or chemical potential field [1, 2]. Since it has been exploited to natural uranium enrichment in 1940s [3], Ceramic Membrane (CM) has been swiftly utilized in whole gamut of water treatments, in virtue of its unique mechanical structures, well chemical stability and long service life [4, 5]. Regarding to Ceramic Membrane Ultrafiltration (CMU) process, one of the potential menace needs to be accentuated is the membrane fouling when CMU filters micro-polluted source water, e.g. reservoir water or pond water that incorporating higher organic matter. Owing to fouling formation, permeate flux attenuates at constant transmembrane pressure, which not only plummets yield efficiency, but also proliferates energy consumption. Albeit meteoric growth of nascent pretreatment techniques were garnered, attempting to mitigate the pollution loading of CMU (e.g., magnetic flocculation [6, 7], electrocoagulation [8-11], advanced oxidation [12], and adsorption [13-

15]). However, delving among membrane fouling is still in an embryonic stage.

Since the antecedent work of Fujishima in 1972 [16], TiO₂ photocatalytic oxidation have engendered extensive attention for its groundbreaking integration of chemical stability and catalytic activity, high adsorption affinity and minimal outlay [17, 18]. When titanium dioxide is illuminated by UV light with energy tantamount to or greater than the band-gap energy, it transfers the photo-generated electrons from the valance band (VB) to the conduction band (CB), resulting in the formation of positive holes (h^+) and the electrons (e^-), respectively [19, 20]. The positive h^+ in the process of UV-TiO₂ photocatalytic oxidation could be applied to mineralize organic pollutants. On the other side, the photo-excited electrons could generate reduced products on the surface of TiO₂. The principal mechanism of UV-TiO₂ photocatalytic reaction is delineated in Fig 1, which normally clarified in three steps: i) photoexcitation of electron-hole pairs; ii) transformation of charge; iii) depletion of charges for redox reactions.

---

*To whom all correspondence should be addressed.
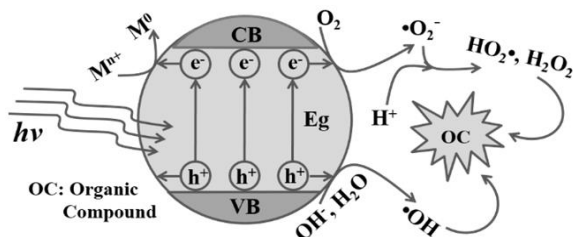
Fig. 1: Mechanism of TiO_2 photocatalytic oxidation.

The powdered TiO_2 requires solid/liquid segregation after reaction, but knowledge concerning the possible segregation method of catalytic titania remains limited hitherto, curbing its widespread industrial applications. Our previous publication [21] displayed the potential of UV/TiO_2-CMU system in enhancement water purification with the respect to effluent quality.

In the light of that mire, we investigate the CMU hybrid system to achieve an ideal combination, including efficient separation and reutilization of catalyst particles, prevention of membrane fouling.

Experimental

Raw water

A typical micro-polluted source water sample was obtained from East Lake in Logistical Engineering University. The detailed water parameters are listed as following, temperature of 25.0-29.0 ℃, pH of 7.6-8.2, turbidity of 7.83-11.22 NTU, COD_{Mn} of 6.06-7.57 mg•L^{-1} as well as UV_{254} of 0.167-0.175 cm^{-1}. During the entire gamut of experimental period, the properties of such original water were similar.

Setup and reagents

A schematic flow diagram of the trial apparatus is sketched in Fig 2. The photocatalytic reactor was fabricated of stainless steel (height=800 mm, inradius=200 mm, and thick=1 mm) with working volume of 22 L. A loop aeration pipe was fixed at the bottom of the photocatalytic cell with a mean pore size of 50 μm. UV (254 nm) radiation is provided by five 37-W lamps (ZW37D15Y(W)-Z793, Cnlight optical-electrical technology Co. Ltd., Guangdong, China).

The ultrafiltration module (crossflow filtering mode, Huicheng water treatment equipment Co. Ltd., Nanjing, China) consists of two series-connected inner driving ceramic membranes (Al_2O_3) with a length of 500 mm. A booster pump (40 m, 2.5 m^3/h, 450 W, Haobei mechanical-electrical equipment Co. Ltd., Shanghai, China) was used to pump the raw water through 37 channels. Then, the water was winnowed by the thin ceramic membrane layer adhered to each raw water channel with nominal aperture of 50 nm. The sifted water was amassed in the filtrate ditches flowed out of the permeated collection grooves, and eventually was stored in a 3 L backwash cylinder and permeate tank under ambient condition. The abovementioned setup consists of an air compressor (JS-2001, Jieshun technology industry Co. Ltd., Shenzhen, China), which was introduced to remove the membrane fouling.

The purchased powder anatase titanium dioxide (99% purity, Sinopharm Chemical Reagent Co. Ltd., Shanghai, China) have D_{50}-values of 46 nm and D_{90}-values of 182 nm, coupling with a specific surface area of 16.9 m^2/g. However, it cannot pass the 50 nm membrane pores because of the aggregation of TiO_2 particles in solution [22-24]. The pH of the TiO_2 suspension was vacillated between 6.8 and 8.0. Sodium hypochlorite, sodium hydroxide, and citric acid were outright acquired from Sinopharm Chemical Reagent Co. Ltd. (Shanghai, China) in analytical grade. All the chemicals were used without further purification.
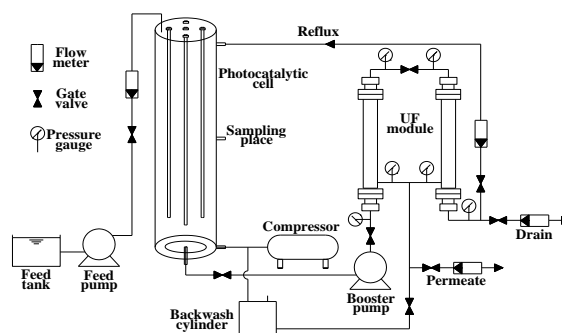
Fig. 2: Schematic flow diagram of experimental configuration.

Trial procedures

Before each test, the required operation parameters were adjusted using tap-water. Initially, the immersible pump (15 m, 3.0 m^3/h, 550 W,

GRUNDFOS) pumped raw water into the feed tank where the lake water mixed with titania powder. Secondarily, a feed pump pulled the admixture into the photocatalytic cell. Concurrently, UV irradiation was offered by five tubs, and the micro-perforated aeration pipe supplied wanted gas flow powered through the air compressor. Then, the post-reaction mixture was injected into the ultrafiltration module through the booster pump. When the permeate streams floated in the backwash cylinder and the permeate tank, the concentrating streams was divided into two sections. One segment of the concentration *i.e.*, retentate streams was reflowed to photocatalytic cell to recycle the TiO_2 photocatalysts and aggrandize the photoreaction time. The other portion of the compression was drained, according to the reflux ratio, which was tuned by the gate valve in the pipeline. Replenish TiO_2 is necessary based on the amount of drained concentrate to maintain a constant TiO_2 concentration. Additionally, the running parameters of transmembrane pressure (TMP) and crossflow velocity (CFV) were modulated through the valve in the outlet of the booster pump and the line of retention.

The yield of permeated water was recorded at 5-minute intervals. After each trial, hydraulic backwashing and chemical circulation cleaning were carried out to regain the membrane permeability in virtue of the air compressor and booster pump. On the heels of hydraulic backwashing, the efficiency of four chemical cleaning strategies [25] were compared: i) online chemical circulation cleaning with oxidant agent (1% NaClO) at TMP of 0.1 MPa for 40 min; ii) online alkali solution (1% NaOH) circulation cleaning at TMP of 0.1 MPa for 40 min; iii) online chelating agent (1% citric acid) circulation cleaning at TMP of 0.1 MPa for 40 min; iv) online chemical circulation cleaning with alkali and chelator at TMP of 0.1 MPa for 20 min respectively.

The cleaning efficiency was evaluated via the membrane flux recovery factor Y (Formula 1) and resistance growth factor Y' (Formula 2).

$$Y = \frac{J}{J_0} \times 100\% \qquad (1)$$

$$Y' = \frac{R - R_0}{R_0} \times 100\% \qquad (2)$$

Here, J is membrane flux before chemical washing, J_o is initial membrane flux of new membrane, R is membrane resistance before chemical washing, and R_o is initial membrane resistance of new membrane.
Membrane resistance model

According to the series model plots in Fig 3, the total resistance (R_t) is assumed to be the sum of the intrinsic membrane resistance (R_m), polarization layer resistance (R_p), deposit resistance (R_e), and internal fouling resistance (R_i) [27, 28].

$$J = \frac{k\Delta P}{\mu R_t} = \frac{k\Delta P}{\mu(R_m + R_p + R_e + R_i)}$$
$$(3)$$

Here, J is membrane flux (L/(m²•h)), ΔP is TMP (Pa), μ is water viscosity (Pa•s), k is constant number (3.6×10^6), R_t is total resistance (m⁻¹), R_m is intrinsic membrane resistance (m⁻¹), R_p is polarization layer resistance (m⁻¹), R_e is deposit resistance (m⁻¹), R_i is internal fouling resistance (m⁻¹).

Those hydraulic resistances were calculated using modified Darcy-Poiseuille Law [27].
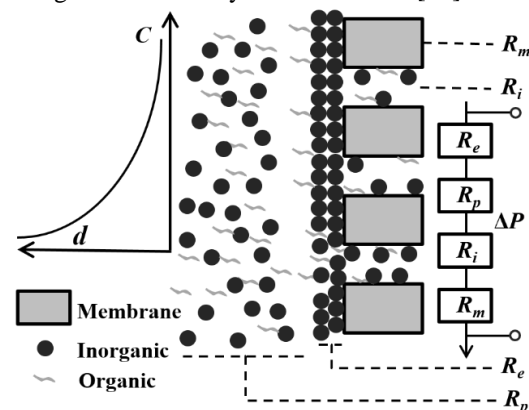
Fig. 3:   Composition of membrane resistances.

Results and Discussion

Single factor experiments

Impact of Aeration Rate. Axiomatically, instable bubbles caused by aeration is advantageous to sweep away concentration polarization on membrane surface. The effect of aeration rates (2-10 L/min) on the membrane flux and membrane resistances is delineated in Fig 4. The performance was compared under the following conditions: reflux rate 85%, TMP 0.05 MPa, CFV 1.5 m/s, and TiO_2 concentration 0.5 g/L.
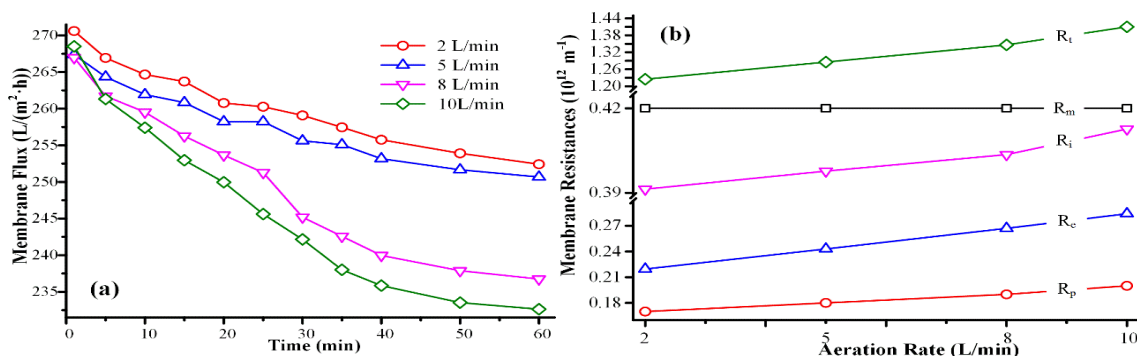
Fig. 4:   (a) Effect of aeration rate on membrane flux. (b) Membrane resistances as a function of aeration rate.

It can be seen from Fig 4 (a) that the membrane flux dwindles as the escalation of aeration rate. And the membrane flux is stemmed by polarization layer, external fouling, and internal fouling during crossflow filtration. Concurrently, Fig 4 (b) presents the increase tendency of membrane resistances *i.e*., R_t, R_p, R_e, R_i. Among all membrane resistances, the R_e remains the major resistance which accounts for 33.78% of total resistance.

It has been widely postulated that the collision strength has greatly increased as the increment of aeration rate, which reduces the size of aggregated TiO_2 and increases R_p slightly. Meanwhile, the reduced TiO_2 aggregations also incubated more compact deposition layer on membrane, and as a consequence, a swelling of the R_e. Concerning the internal fouling, the impact of

aeration has two sides. On one hand, the escalation of aeration aggrandized the reaction extent of photocatalysis leading the inadequate photodegraded small-sized intermediate ingress membrane pores easily; on the other hand, such intermediate also could be intercepted by the compact deposition fabrics. Overall, in this case, the former effect outdid the latter one. Thus the R_i manifested a modicum of growth.

Impact of TiO_2 concentration. The impact of TiO_2 concentration (0.3, 0.5, 0.8, 1.1 g/L) was tested under the idential circumstances: CFV, 1.5 m/s; TMP, 0.05 MPa; aeration rate, 5 L/min; reflux rate, 85%. The membrane flux and corresponding membrane resistances with a TiO_2 suspension concentration range from 0.3 to 1.1 g/L are shown in Fig 5 (a) and (b).
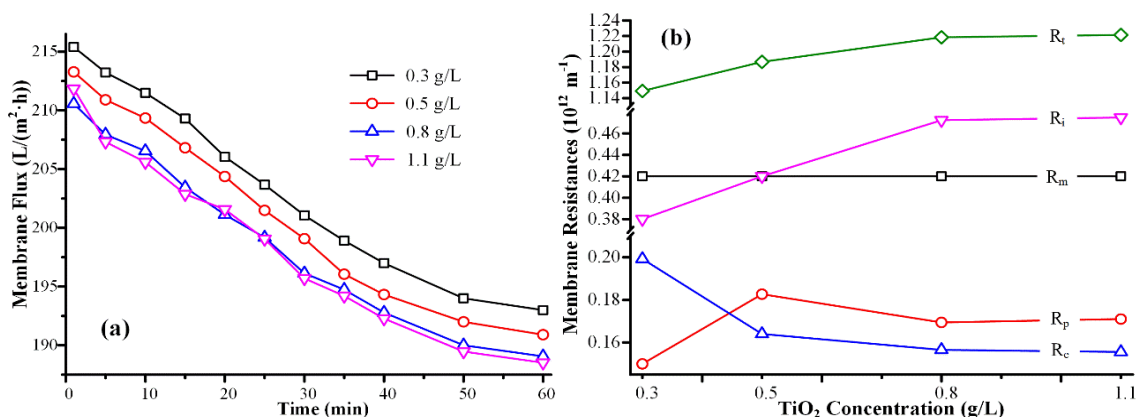
Fig. 5:   (a) Effect of TiO_2 concentration on membrane flux. (b) Membrane resistances as a function of TiO_2 concentration.

Form the observation of Fig 5(a), it is unambiguous that membrane flux downgrade rapidly within the purview of 0.3-0.8 g/L TiO_2 and then decline gently after 0.8 g/L. Results from the reaction process show that the internal fouling resistance (R_i) manifest a sharp improvement with the increment of TiO_2 concentration before 0.8 g/L, hereafter reaching a plateau. Intriguingly, the polarization layer resistance (R_p) demonstrates an undulating phenomenon: swelling sharply in the range of 0.3-0.5 g/L, then diminishing within the sphere of 0.5-0.8 g/L, and heaving slightly hereafter. Conversely, the deposit resistance (R_e) shows a downward tendency in the test condition.

The culprit was pertinent to the adsorptive power between TiO_2 aggregations. In accordance with the kinetic theory of Langmuir-Hinshelwood, the photocatalytic oxidation could be rend into two stages, *i.e.*, adsorptive accumulation and oxidative degradation. The rate-limiting step lie in the former one, which accentuated adsorption rate was vital in the TiO_2 photocatalytic oxidation [28]. The electrostatic attraction plays an important role in the reaction between TiO_2 particles and organic contaminants. It is generally postulated that TiO_2 is an amphoteric oxide. As was depicted in Formula 4, massive groups of $\equiv TiOH$ was formed by coordination in hydrolysis [29].

$$pH<pH_{zpc} \quad \equiv TiOH_2^+ \leftrightarrow \equiv TiOH + H^+$$
$$pH>pH_{zpc} \quad \equiv TiOH \leftrightarrow \equiv TiO^- + H^+ \quad (4)$$
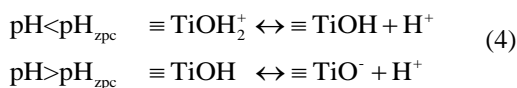
The hydrolyzed $\equiv TiOH$ resemble to a dibasic acid. As the pH value of the solution (pH>7.5) outstripped the isoelectric point of TiO_2 (pH_{zpc}=6.3), the dominant product of the reaction was TiO^-. Furthermore, according to Formula 5, the process of photocatalytic oxidation is a pH-dropping procedure in the wake of OH^- depletion and H^+ production [30].

$$h^+ + OH^- \rightarrow \bullet OH$$
$$h^+ + H_2O \rightarrow \bullet OH + H^+ \quad (5)$$

Whereas the results of Yan attested that the pH of the post-reaction solution maintained to ca. 7.0 [31]. Therefore, anatase TiO_2 surface loaded negatively charged in the slightly alkaline solution and tended to the isoelectric point as the reaction progress. Thus, TiO_2 particles were apt to agglomerate for the weaker repulsive force, incubating a loose deposit layer [32].

Moreover, Carman-Kozeny equation demonstrates that the value of deposit resistance (Re) is directly proportional to specific resistance of filter cake (α) when TMP and CFV are constant [33]. The equation can be expressed as follows:

$$\alpha = \frac{180(1-\varepsilon)}{\rho_p d_p^2 \varepsilon^3} \quad (6)$$

Here, ρ_p is the density of particles, d_p is the grain size of particles, ε is the porosity of sedimentary layer.

Accordingly, the additional TiO_2 concentration accelerated the photocatalysis process and dwindled the pH value in the sphere of 0.3-0.8 g/L, dropping the R_e with the rise of ε and d_p. When the structure of deposit layer becomes looser, the intermediate was more accessible to enter into the porous medium, resulting in a higher internal fouling resistance (R_i). Contrariwise, the plethora of TiO_2 concentration (>0.8 g/L) was pernicious to photocatalytic reaction rate for the robust scattering effect by excessive TiO_2 particles, resulting a relatively compact sediment layer and a plateau of R_i. What's more, the baneful influence of excessive TiO_2 also embodied in the weaker mass transfer coefficient which trifling inflated the polarization layer resistance (R_p).

Thereupon, the catalysis content of TiO_2 photocatalytic oxidation pretreatment not attenuated CMU flux severely within the purview of 0.3-1.1 g/L, in line with Lee's assertion [34].

Impact of transmembrane pressure. The influence of TMP on filtrate flux and membrane resistances was delved into with TMP of 0.05, 0.10, 0.15, and 0.20 MPa. The following working conditions were adopted in the test: CFV, 1.5 m/s; TiO_2 concentration, 0.5 g/L; aeration rate, 5 L/min; reflux rate, 85%.

Based on Formula 3, TMP is a crucial driving force in CMU process. From Fig 6(a), it is clear that the membrane flux rise as an increment of TMP. However, such improvements in flux dwindled after 0.15 MPa. The meteoric growth of membrane resistances in Fig 6(b) chimed with that flux attenuation phenomenon. Such opposite effect of TMP can be attributed to the undulation of retention period and concentration polarization. When TMP lie in the initial level, retention period will be extended and photocatalysis reactivity will be promoted. Both of them induced a loose TiO_2-based deposit layer on membrane surface, coupling well permeability.
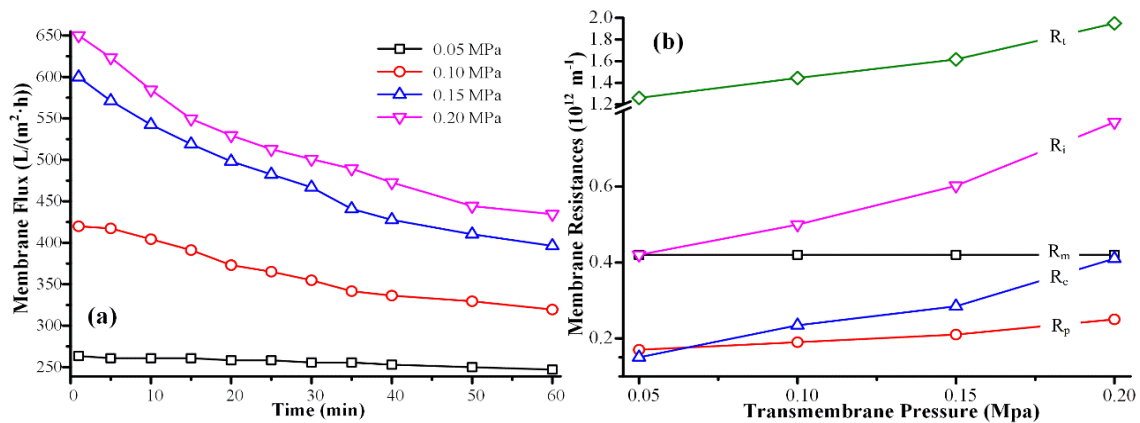
Fig. 6:   (a) Effect of TMP on membrane flux. (b) Membrane resistances as a function of TMP.

As TMP increases, the system needs more input of original water. The organic particle has more probability to penetrate through the porous medium and incubate internal fouling (R_i). Secondarily, more pollutants congregated in the vicinity of the membrane surface, proliferating the concentration of the boundary layer and causing a severe concentration polarization (*i,e,,* swelling the R_p). Likewise, concerning R_e, increasing TMP actuated the settling of sediment and plummeting its porosity, even forming a compact gel.

Moreover, higher TMP restrained the retention period in the reactor. And the insufficient reaction degree swelled the loads of CMU. When the improvements of flux via the escalation of TMP cannot match the attenuation causing by membrane fouling, its throughput decreased rapidly [35].

Impact of Crossflow Velocity. It has been widely postulated that CFV is a paramount running

parameter for the filtration of real micro-polluted surface water. Its positive effect is ascribed to the shearing stress which manipulate the deposit thickness and diffusion layer. For example, the polarization layer resistance (R_p) hinged on diffusion layer thickness, which is inversely proportional to CFV.

Fig 7 delineates the variability of membrane flux and resistances with the different CFV (1.0-2.5 m/s) values under identical conditions: TMP, 0.1 MPa; TiO_2 concentration, 0.5 g/L; aeration rate, 5L/min; reflux rate, 85%. From the observation of Fig 7(a), it is unambiguous that the amplification of membrane flux upgraded rapidly in the range of 1.0-2.0 m/s (12.2%, from 301.25-339.87 L/(m^2•h)) at 60 min. While the increment rate of membrane resistance from 2.0 m/s to 2.5 m/s at 60 min only occupied 1%.
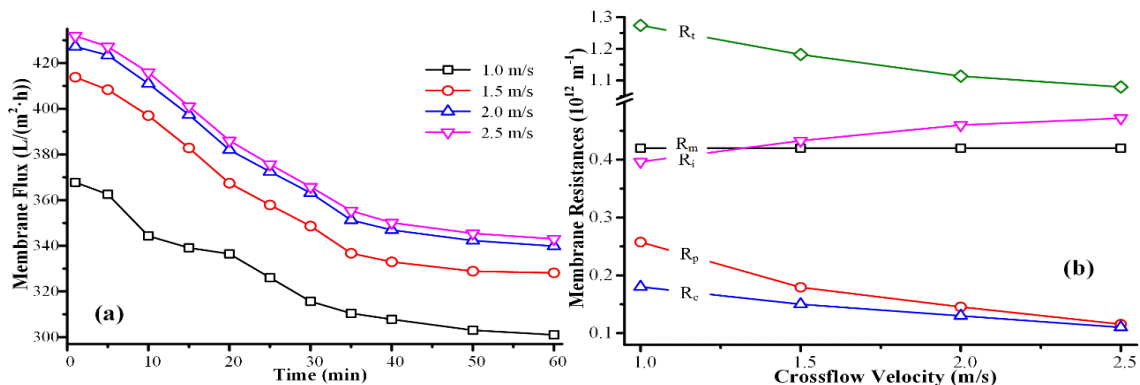
Fig. 7:   (a) Effect of CFV on membrane flux. (b) Membrane resistances as a function of CFV.

Lower CFV and weaker shearing stress, in the primary stage, were accountable for the knot of the matter, which resulted in the higher R_e and R_p. In contrast, when the integrated process entry into the higher CFV running stage, the flux attenuation were be mitigated because of the escalation of local mixing and tangential fluid flow which crippled the thickness of the boundary layer and alleviated the concentration polarization [36, 37].

However, it is worth emphasizing that unduly mighty shearing stress may bring about a thinner deposit layer, smaller pollutant aggregation, and even shatter the sediment layer. Furthermore, increasing trapped pollutants were attached to the membrane pores as the rising of influent water quantity [38]. What's more, due to the insufficient photoreaction time, the photodegradation of pollutant was inadequate. These aftermaths expedited the internal fouling (R_i) and flux decline.

Orthogonal methodology optimization

Herein, orthogonal methodology was introduced to optimize operating variables based on the aforementioned single factor analysis. Orthogonal test was implemented considering four factors (TiO$_2$ concentration, aeration rate, TMP and CFV) at three levels, as tabulated in Table-1.

Table-1: Factors and levels in orthogonal methodology at the response value of membrane flux.

Factors / Level	A/TiO$_2$ Concentration g/L	B/aeration rate L/min	C/TMP MPa	D/CFV m/s
1	0.3	2	0.05	1.0
2	0.5	5	0.10	1.5
3	0.8	8	0.15	2.0

Comparatively stable membrane flux was recorded in Table 2.

The data demonstrates that the impact of those operating parameters can be listed in the order of $R_C > R_D > R_B > R_A$. Moreover, the optimum operating condition was the combination of $C_3D_3B_1A_2$, which was selected on the basis of K_{ij} (i=1,2,3; j=1,2,3,4) values.

Table-2: Results of the orthogonal experiment at the response value of membrane flux.

No.		A/TiO$_2$ concentration g/L	B/aeration rate L/min	C/TMP MPa	D/CFV m/s	Membrane flux L/(m^2·h)
1		0.3	2	0.05	1.0	185.01
2		0.3	5	0.10	1.5	261.69
3		0.3	8	0.15	2.0	480.53
4		0.5	2	0.10	2.0	380.38
5		0.5	5	0.15	1.0	390.42
6		0.5	8	0.05	1.5	228.66
7		0.8	2	0.15	1.5	448.62
8		0.8	5	0.05	2.0	242.57
9		0.8	8	0.10	1.0	260.83
	K_1	309.08	339.00	218.75	278.75	
Membrane flux	K_2	333.15	298.23	300.97	312.99	
	K_3	317.34	323.34	439.85	367.83	
	R	24.07	39.77	221.10	89.08	

Table-3: ANOVA table for membrane flux.

Source	Sum square	Freedom degrees	F-value	Critical value	Significance
TiO$_2$ concentration	898.03	2	105.28		***
Aeration rate	2427.88	2	248.53	$F_{0.1}(2, 2)=9.00$	***
TMP	74940.32	2	8785.27	$F_{0.05}(2, 2)=19.00$	***
CFV	12113.43	2	1420.04	$F_{0.01}(2, 2)=99.00$	***
Error	8.53				

The variance analysis of test data was tabularized in Table 3. It is distinct that all four sources possessing "***" in the sixth column of Table 3 are highly significant at 95% confidence level to membrane flux.

Comparison with chemical coagulation pretreatment

The stability and reliability of the hybrid technique was inspected in long-time continuous operation with the aforementioned optimum parameters. Additionally, the performance of pre- coagulation and oxidation was compared in their corresponding optimal conditions (Fig 8). In terms of chemical coagulation-CMU integrated process, polyaluminum chloride (PAC) was adopted as flocculant in virtue of its wide adaptability to pH, which has a slight influence on effluent quality, etc.; In addition, Feng [39] and Zhu [40] asserted that the ideal PAC concentration to pond water treatment was in the range of 20-30 mg/L. What's more, Xie [38] attested that excellent filtration capacity was emerged during CMU (with pore size of 50 nm) micro-polluted surface water treatment process in 2.0 m/s CFV, 0.15 MPa TMP. Based on these, the controlled variables of chemical coagulation combined CMU hybrid process were selected as follows: PAC concentration, 25 mg/L; TMP, 0.15 MPa; CFV, 2.0 m/s.

Herein, the sum of R_p and R_e was denoted as reversible fouling resistance (R_r) during the long-time continuous test to evaluate the ability of these two pretreatment technologies [41]. Moreover, 40 min was chosen as the backwashing cycle according to our previous study [42]. Therefore, time dependent membrane flux between pre- coagulation and oxidation is sketched in Fig 8.

The hybrid process of TiO$_2$ photocatalytic oxidation-CMU approximately reached a steady-state stage after 120 min ultrafiltration. Henceforward, the fluctuation range of membrane flux in each cycle was negligible. On the contrary, the steady-state flux to the chemical coagulation pretreatment system was always inferior to oxidation pretreatment and the fluctuation range of the former outdid the corresponding later.
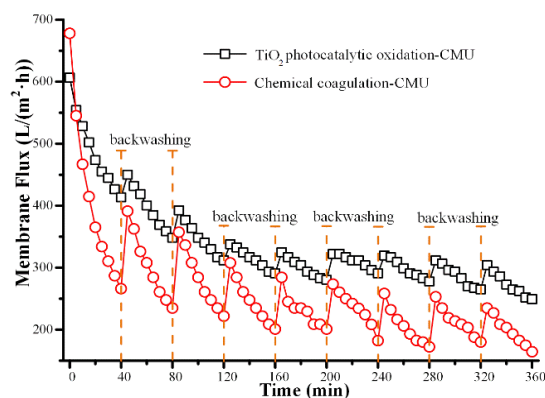
Fig. 8: Effect of coagulation and photocatalytic pretreatments on CMU flux.

Fig 9 sketches the change of membrane resistances as a function of filtration time in these two combined techniques. It reveals that the value of R_t in Fig 9(a) was much less than that in Fig 9(b) and the value of R_r and R_i in the pre-oxidation process were lower than pre-coagulation process.
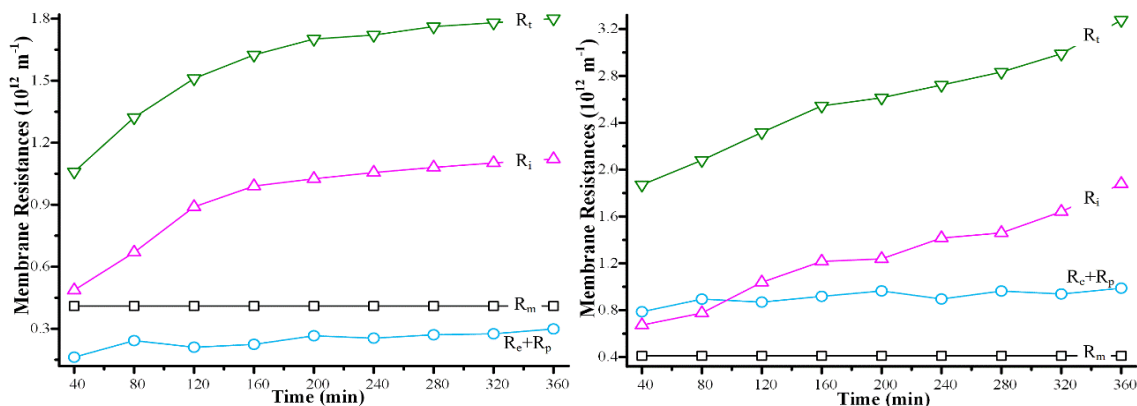
Fig. 9:   (a) Variation of membrane resistances by photocatalytic oxidation-CMU process. (b) Variation of membrane resistances by coagulation-CMU process.

In Fig 9(a), the reversible resistance only constitutes circa 15% of total resistance during the entire ultrafiltration process, which attributed to the photodegradation of organic compound and alleviated the pollution loading. Of note, titania particles aggregated and generated fairly large agglomerates, and then a hydrophilic porous cake layer yielded on membrane facet, which was beneficial to low-level reversible resistance [43, 44].

Concerning internal fouling resistance, the meteoric growth of R_i in the pre-coagulation process was ascribed to micro-molecular organics, which was prone to enter into membrane hole. Furthermore, the inferior performance of PAC to neutral organic matters also incriminated to such severe internal fouling. However, the counterpart swiftly garnered a relatively compact deposit layer on the membrane surface as the addition of TiO$_2$ particles, which effectively stemmed the aggravation of internal fouling.

Overall, abovementioned evidence stated TiO$_2$ photocatalytic oxidation-CMU process was superior to PAC based chemical coagulation-CMU technique in mitigating flux attenuation.

Chemical cleaning

Membrane fouling may be mitigated, but inevitable during the process of filtration [45]. Accordingly, we investigated the reinstatement ability of four different chemicals (*i.e.*, NaClO, NaOH, citric acid, and NaOH+citric acid) on membrane fouling. Variations of the membrane flux recovery factor and the resistance growth factor are plotted in Fig 10.

It clearly reveals that citric acid possesses superb reinstatement capacity for membrane fouling after 40 min rinse. It is well documented that different chemical agents target on different membrane fouling: alkaline solution (NaOH) is relatively effective for the elimination of organic fouling, oxidizing agent (NaClO) is advantageous to control bio-fouling, while inorganic fouling is apt to be obviated in the presence of cheating agent (citric acid) [2, 25]. Thus, in this ultrafiltration process of micro-polluted surface water, the major irreversible resistance stemmed from the inorganic compound and can be effective eliminated via citric acid.

Conclusion

To mitigate membrane flux attenuation during micro-polluted surface water ultrafiltration process, herein, we investigated TiO$_2$ photocatalytic oxidation-CMU composite technique. The fundermental results were assembled as followings:

i. The significance on permeate flux was manifested in the order of TMP>CFV>aeration rate>TiO$_2$ concentration. The hybrid process attained the orthogonal optimized membrane flux under the parameters of: aeration rate, 2 L/min; TMP, 0.15 MPa; CFV, 2.0 m/s; TiO$_2$ concentration, 0.5 g/L.

ii. The membrane flux enhancement of TiO$_2$ photocatalytic oxidation pretreatment outdid PAC based chemical coagulation pretreatment.

iii. The maximized membrane permeability reinstatement was achieved during 40 min citric acid cycle-washing.
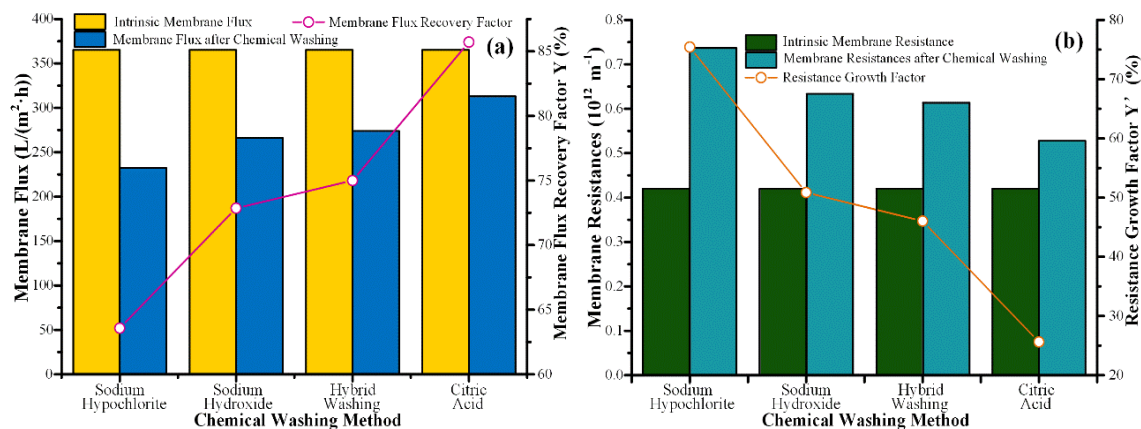
Fig. 10:   (a) Effect of chemical washing on the recovery of membrane flux and recovery factor. (b) Effect of chemical washing on membrane resistances and growth factor.

Acknowledgements

References

1. Y. L. Tian, G. Z. Liu, Y. Q. Yang, C. J. Gao, and D. D. Yuan, Research on Inorganic Membrane Separation Technology Application in the Field Of Water Treatment, *Environ. Prot. Sci.*, **37**, 16 (2011).

2. Z. Zhou, J. L. Yao, Z. B. Pang, and B. Liu., Research Progress on Performance Change of Ceramic Membrane for Water Treatment, *Chem. Bioeng.*, **33**, 1 (2016).

3. R. R. Bhave, In *Inorganic Membranes Synthesis, Characteristics and Applications*, New York: Van Nostrand Reinhold, p. 1 (1991).

4. G. Meng, C. Chen, and W. Liu, Ceramic Membrane Technology: 30 Years Retrospect and Prospect, *Membr. Sci. Technol.*, **31**, 86 (2011).

5. Y. Cao, H. Xu, and J. Wang, Development Status and Prospect of Inorganic Ceramic Membrane in China, *Membr. Sci. Technol.*, **33**, 1 (2013).

6. Z. B. Pang, J. L. Yao, B. Liu, and Z. Zhou, Experimental Study on Treatment of Micro Polluted Raw Water by Combined Process of Magnetic Flocculation and Membrane Filtration, *Technol. Water Treat.,* **42**, 21 (2016).

7. Z. B. Pang, J. L. Yao, B. Liu, and Z. Zhou, Optimization of Magnetic Flocculation and Membrane Filtration Process with Response Surface Method, *J. Logistical Eng. Univ.*, **32**, 62 (2016).

8. Z. Zhou, J. L. Yao, Z. B. Pang, and B. Liu, Mitigated Fouling of Ceramic Microfiltration Membrane by Electrocoagulation Pretreatment, *Chin. J. Environ. Eng.*, **10**, 2279 (2016).

9. Z. Zhou, J. L. Yao, Z. B. Pang, and B. Liu, Optimization of Electrocoagulation-Ceramic Micro-Filtration Membrane Process by Response Surface Method, *Environ. Pollut. Control,* **38**, 39 (2016).

10. Z. Zhou, J. L. Yao, Z. B. Pang, and B. Liu, Optimization of Electrocoagulation Process to Eliminate UV_{254} in Micro-Polluted Surface Water using Response Surface Method, *Technol. Water Treat.*, **42**, 32 (2016).

11. Z. Zhou, J. L. Yao, Z. B. Pang, and B. Liu, Optimization of Electrocoagulation Process to Eliminate COD_{Mn} in Micro-Polluted Surface Water using Response Surface Method, *J. Dispersion Sci. Technol.*, **37**, 743 (2016).

12. D. S.Bhatkhande, V. G. Pangarkar, and A. A. Beenackers, Photocatalytic Degradation for Environmental Applications-A Review, *J. Chem. Technol. Biotechnol.*, **77**, 102 (2002).

13. M. Zahoor, Removal of Synthetic Organic Foulants by Granular Activated Carbon Filters and Ultrafiltration Membrane, *Tenside Surfactants Deterg.*, **49**, 382 (2013).

14. M. Zahoor, Removal of Paraquat and Linuron from Water by Continuous Flow Adsorption/ Ultrafiltration Membrane Processes, *J. Chem. Soc. Pak.*, **35**, 577 (2013).

15. M. Zahoor, Magnetic Adsorbent Used in Combination with Ultrafiltration Membrane for the Removal of Surfactants from Water, *Desalin. Water Treat.*, **52**, 3104 (2014).

16. A. Fujishima, and K. Honda, Electrochemical Photolysis of Water at A Semiconductor Electrode, *Nature*, **238**, 37 (1972).

17. N. U. Saqib, R. Adnan, and I. Shah, A Mini-review on Rare Earth Metal-Doped TiO_2, for Photocatalytic Remediation of Wastewater, *Environ. Sci. Pollut. Res.*, **23**, 15941 (2016).

18. T. Jafari, E. Moharreri., A. S. Amin, R. Miao, W. Song, and S. L. Suib, Photocatalytic Water Splitting-the Untamed Dream: A Review of Recent Advances, *Molecules*, **21**, 1 (2016).

19. R. Thiruvenkatachari, S. Vigneswaran, and I. S. Moon, A Review on UV/TiO_2, Photocatalytic Oxidation Process, *Korean J. Chem. Eng.*, **25**, 64 (2008).

20. M. M. Mahlambi, C. J. Ngila, and B. B. Mamba, Recent Developments in Environmental Photocatalytic Degradation of Organic Pollutants: the Case of Titanium Dioxide Nanoparticles-A Review, *J. Nanomater.*, **2**, 1 (2015).

21. Z. Zhen Y. J. Lun, Z. Xing, D. Zhao. Xia, and Z. M. Mei, Enhanced effluent quality of ceramic membrane ultrafiltration combined with UV/TiO_2 photocatalysis, *Nat., Environ. Pollut. Technol.*, **16**, 695 (2017).

22. L. Lei, N. Lu, and M. Wu, De-aggregation of Nano-TiO_2 Soft Agglomeration in Aqueous Medium, *Chin. J. Chem. Eng.* **60**, 3159 (2009).

23. H. Hua, Ph.D. Thesis, Study of Photocatalysis-Membrane Filtration Integrate Process, Nanjing University of Science and Technology at Nanjing, (2006).

24. X. Weimin, and G. Sven-Uwe, Separation of titanium Dioxide from Photocatalytically Treated Water by Cross-Flow Microfiltration, *Water Res.*, **35**, 1256 (2001).

25. W. Zhang, L. Ding, J. Luo, Y. J. Michel, and T. Bing, Membrane Fouling in Photocatalytic Membrane Reactors (PMRs) for Water and Wastewater Treatment: A Critical Review, *Chem. Eng. J.*, **302**, 446 (2016).

26. M. Ousman, and M. Bennasar, Determination of Various Hydraulic Resistances during Cross-Flow Filtration of a Starch Grain Suspension through Inorganic Membranes, *J. Membr. Sci.*, **105**, 1 (1995).

27. M. Marcel, In *Basic Principles of Membrane Technology (2th ed)*, Holland: Kluwer Academic Publishers, p. 270 (1996).

28. J. Fu, M. Ji, and L. Jin, Factors Affecting Degradation of Acid Blue 7 by using Photocatalysis-Ultrafiltration Separation Reactor, *Chem. Ind. Eng. Prog.*, **24**, 916 (2005).

29. Y. Jiang, Ph.D. Thesis, *Modification of TiO_2/Ti catalyst and Its Photoelectric Catalysis Degradation of Humic Acid in Water*, Harbin Institute of Technology at Harbin, (2007).

30. M. C. Cathy, S. Nathan, A. Morgan., and P. K. J. Robertson, Photocatalytic Reactors for Environmental Remediation: A Review, *J. Chem. Technol. Biotechnol.*, **86**, 1002 (2011).

31. X. Yan, Ph.D. Thesis, *Research on the Performance and the Mechanism of Humic Acid Removal by the Photo*catalysis-*Membrane Integrated Process*, Harbin Institute of Technology at Harbin, (2009).

32. H. Zhang, Ph.D. Thesis, *Photocatalysis and Membrane Separation Hybrid System Used in Dyeing Wastewater Treatment and Reutilization*, Zhejiang University of Technology at Zhejiang, (2010).

33. K. M. Boerlage, Applications of the MFI-UF to Measure and Predict Particulate Fouling in RO Systems, *J. Membr. Sci.*, 220, 97 (2003).

34. S. Lee, K. Choo, C. Lee, H. Lee, T. Hyeon, W. Choi, and H. Kwon, Use of Ultrafiltration Membranes for the Separation of TiO_2 Photocatalysts in Drinking Water Treatment, *Ind. Eng. Chem. Res.*, **40**, 1712 (2001).

35. N. Xu, W. Xing, and Y. Zhao, In *Separation Technology and Application of Inorganic Membrane*, Chemical Industry Press, Beijing, p. 9 (2003).

36. P. Li., C. Xie, N. Zhou., L. Chen, and S. Liu, Research on Influence of Pre-Coagulation and Cross-Flow Velocity on Membrane Fouling of Microfiltration, *Environ. Sci. Technol.*, **28**, 1 (2015).

37. Y .He, G. M. Li, H. Wang, J. Zhao, H. Sun, and Q. Huang, Effect of Operating Conditions on Separation Performance of Reactive Dye Solution with Membrane Process, *J. Membr. Sci.*, **321**, 183 (2008).

38. Y. Xie, Ph.D. Thesis, *Study on Ceramic Membrane Filtration and Its Combination with Oxidation for Treatment of Micro-Polluted Water*, Tsinghua University, (2010).

39. M. Feng., Ph.D. Thesis, *Enhanced Coagulation to Micro-Polluted Source Water Treatment*, Wuhan University of Science and Technology, (2005).

40. F. Zhu, Ph.D. Thesis, *Experimental Research on the Treatment of Micro-Polluted Water with Pretreatment-Micro-Filtration Membrane Process*, Nanchang University, (2012).

41. M. Yazdanshenas, M. Soltanieh, S.Nejad, and L. Fillaudeau, Cross-flow Microfiltration of Rough Non-Alcoholic Beer and Diluted Malt Extract with Tubular Ceramic Membranes: Investigation of Fouling Mechanisms, *J. Membr. Sci.,* **362**, 306 (2010).

42. B. Liu., J. L. Yao, Z. B. Pang, and Z. Zhou, Study on Micro-Pollution Water with Photocatalytic Oxidation-Ceramic Ultrafiltration Membrane, *J. Logistical Eng. Univ.*, **32**, 68 (2016).

43. T. H. Bae, and T. M. Tak, Effect of TiO_2, Nanoparticles on Fouling Mitigation of Ultrafiltration Membranes for Activated Sludge Filtration, *J. Membr. Sci.*, **249**, 5 (2005).

44. S. S. Madaeni, and N. Ghaemi, Characterization of Self-Cleaning RO Membranes Coated with TiO_2 Particles under UV Irradiation, *J. Membr. Sci.*, **303**, 221 (2007).

45. Y. Watanabe, and K. Kimura, In *Membrane Filtration in Water and Wastewater Treatment*, Amsterdam: Elsevier, p. 23 (2011).